Stability Analysis and Testing of the High-Speed Active Magnetic Bearing-Flywheel System in the Rotating Frame

Jinpeng Yu [a], Lei Zhao [a], Kai Zhang [b], Pingfan Liu [a], Yanbao Li [c], Pengcheng Pu [a], Yan Zhou [a]

[a] Institute of Nuclear and New Energy Technology, Tsinghua University
[b] Department of Engineering Physics, Tsinghua University
[c] Shanghai Aerospace Control Technology Institute

Abstract*—The active magnetic bearing (AMB) can greatly improve the stability of the flywheel system and increase the maximum flywheel speed. However, if the frame of active magnetic bearing-flywheel system (AMB-FS) rotates in the different direction from the flywheel, the strong gyroscopic effect of high-speed flywheel will greatly affect the system stability. In this study, to realize the high stability of the AMB-FS at ultra-high flywheel speed with low power consumption, the main purpose and content are implementing active control to the strong gyroscopic effect caused by the rotating frame and suppressing the precession and nutation of the flywheel. Through the stability analysis, AMB controller design, simulation and dynamic experiment, the AMB-FS is designed and studied, and the system stability is analyzed in the experiment. In the experiment, the gyroscopic effect of the flywheel is effectively suppressed. In the vacuum environment, the flywheel can be suspended stably at any speed within the range of 0 *to* 30000 rpm*, and the AMB-FS has the power consumption of* 17.82 W *and needs no cooling measures The flywheel speed could exceed* $31200\ rpm$ *and still possess the speeding potential.. The ultimate performance test shows that the maximum frame rotational speed can reach* $3.5\ deg/s$ *at the rated flywheel speed of* 30000 rpm*, and the AMB-FS shows high stability.

INTRODUCTION

The flywheel system is widely applied in uninterrupted power supply (UPS), power conditioning system and spacecraft attitude control system [1-3]. However, the flywheel system supported by mechanical bearings inevitably suffers from the problems of wear, noise, vibration, etc., which will greatly reduce the stability of the flywheel system and limit the maximum flywheel speed. Compared with conventional mechanical bearings, active magnetic bearing (AMB) has no mechanical contact, no lubrication, low noise, long life, etc. Therefore, the active magnetic bearing-flywheel system (AMB-FS) can greatly improve the system stability and increase the maximum flywheel speed.

However, the AMB-FS is a nonlinear system with multiple coupling variables. The rotor imbalance, gyroscopic effect and external disturbance will bring about strict control requirement for the AMB and complicate the control system. Especially in the high-speed AMB-FS, the strong gyroscopic effect of the flywheel will impose a great burden on the AMB and bring about the problem of stability and stability margin [4-5]. The gyroscopic effect will affect the suspension stability seriously and decrease the robustness of the decentralized PID controller significantly. As a result, the AMB controller will fail to meet the control requirements and only small external disturbance acting on the high-speed flywheel will lead to the instability of the AMB-FS.

Combining PID controller with other control methods can achieve good control performance. Displacement cross feedback and speed cross feedback can suppress the gyroscopic effect of the flywheel significantly [6-7], and the notch filter can suppress the flywheel flexible mode [8]. Ahrens [6] used both LQR control and cross feedback control to improve the stability of the AMB-FS. Zhao [9] suppressed the precession frequency of the flywheel effectively with displacement cross feedback control, and presented the experimental results. Horiuchi [10] designed $H\infty$ controller for a large-scale AMB-FS and achieved high-speed and stable operation of the system. Based on robustness control, Li [11] proposed a smooth-switching controller with bidirectional non-jumping transfer method, which achieved the flywheel stability in a large range of speed. Using the LMI method, Sivioglu [12] designed an $H\infty$ controller with gain adjustment, which could suppress the gyroscopic effect significantly. Studies in [13-15] combine variable gain controller with other control methods to stabilize the AMB-FS. Tian [16] proposed a gain-expected cross feedback controller, which set up different gain and bandwidth parameters for cross feedback channel in correspond to different flywheel speed.

With the frame of AMB-FS rotating in the different direction from the flywheel, the strong gyroscopic effect of high-speed flywheel will greatly affect the system stability. Therefore, to realize the high stability of the AMB-FS at ultra-high flywheel speed with low power consumption, the main purpose and content in this study are implementing active control to the strong gyroscopic effect caused by the rotating frame and suppressing the precession and nutation of the flywheel. Based on the vertical AMB-FS with the frame rotating horizontally, the system stability is analyzed and tested in the experiment. In the second section, the flywheel stability and cross feedback PID controller is analyzed and designed on the basis of the AMB-FS structural parameters. In the third section, the stability of AMB-FS under cross feedback PID control is simulated in Matlab Simulink. The stability experiment for high-speed AMB-FS is presented in section four.

STABILITY ANALYSIS AND CONTROLLER DESIGN

For the high-speed AMB-FS, if the frame of the system rotates at a certain speed in the different direction from the flywheel, the gyroscopic effect of the high-speed flywheel will impose a great burden on the AMB, which will seriously affect the flywheel stability and raise strict control requirements for the AMB. Therefore, for the AMB-FS, the rotating frame can also be equivalent to the external disturbance. In this section, based on the vertical AMB-FS with the frame rotating horizontally, the system stability is analyzed.

A. Stability Analysis

In this study, the AMB-FS mainly includes flywheel, frame, AMB system, drive motor, and other appended structures. The three-dimensional structure of the AMB-FS is shown in Fig 1. The system has an inner rotor structure with the radial AMB mounted on the outside of the flywheel, which achieves high inertia ratio of 1.93. The rated flywheel speed is 500 Hz.

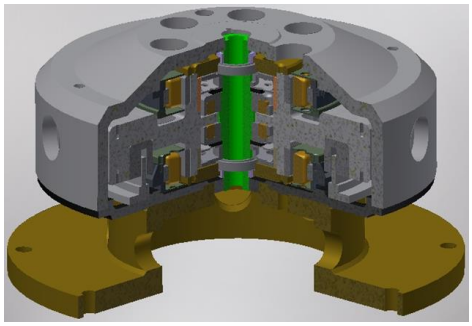

Figure 1. Three-dimensional structure of the AMB-FS.

Neglecting the influence of the flexible modes of the flywheel, the rigid body model and the force conditions are shown in Fig 2. The high-speed flywheel is placed vertically. Since the radial and axial AMB in the system is decoupled, only the radial AMB is analyzed.

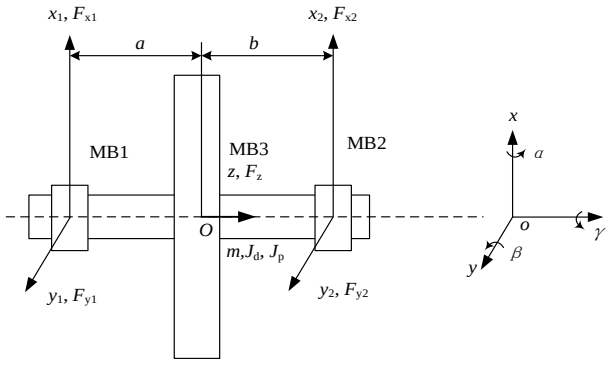

Figure 2. The flywheel model and the force condition.

$\mathrm{MB_i}(i = 1,2)$ are the radial AMB. The flywheel coordinate is $q = [x, \beta, y, -\alpha]^T$ and the AMB coordinate is $q_b = [x_1, x_2, y_1, y_2]^T$, which have the transformation relation $q_b = L_q q$, where

$$L_q = \begin{bmatrix} 1 & -a & 0 & 0 \\ 1 & b & 0 & 0 \\ 0 & 0 & 1 & -a \\ 0 & 0 & 1 & b \end{bmatrix} \tag{1}$$

The distance between the AMB and the flywheel centroid is a and b. In order to simplify the calculation, it is considered that the displacement sensors and the AMB have the same position. In the stationary coordinate system, the motion differential equation of the flywheel is

$$\begin{cases} m\ddot{x} = F_{x_1} + F_{x_2} \\ m\ddot{y} = F_{y_1} + F_{y_2} \\ J_d\ddot{\alpha} = aF_{y_1} - bF_{y_2} - J_p\Omega\dot{\beta} \\ J_d\ddot{\beta} = -aF_{x_1} + bF_{x_2} + J_p\Omega\dot{\alpha} \end{cases} \tag{2}$$

with m the mass of flywheel, x and y the displacements of the flywheel centroid, α and β the rotation angles in the x and y directions, J_d and J_p the diameter and polar moment of inertia and Ω the flywheel speed. F_{x_1}, F_{x_2}, F_{y_1} and F_{y_2} are the electromagnetic forces acting on the flywheel.

The motion differential equation of the AMB-FS can be rewrite in matrix form

$$M\ddot{q} + G\dot{q} = L_F F \tag{3}$$

where $M = diag(m, J_d, m, J_d)$, $F = \left[F_{x_1}, F_{x_2}, F_{y_1}, F_{y_2}\right]^T$, $L_F = L_q^T$ and

$$G = \begin{bmatrix} 0 & 0 & 0 & 0 \\ 0 & 0 & 0 & 1 \\ 0 & 0 & 0 & 0 \\ 0 & -1 & 0 & 0 \end{bmatrix} J_p\Omega \tag{4}$$

Let $I = diag(1,1,1,1)$.The AMB force can be linearized as $F = K_x q_b + K_i I_c$, where $K_x = k_x I$ and $K_i = k_i I$ are force-displacement and force-current stiffness matrices respectively. Under PD current feedback control, the AMB current is

$$I_c = -\left(K_p G_s G_i q_b + K_d C G_s G_i \dot{q}_b\right) \tag{5}$$

where $G_s = g_s I$ and $G_i = g_i I$ the coefficients of the displacement sensor and power amplifier, $K_p = k_p I$ and $K_d = k_d I$ the parameter matrices of the PD controller. The matrix C is the cross feedback coefficient. Substitute the AMB force into Equ (3) and obtain Equ (6)

$$M\ddot{q} + N\dot{q} + Rq = 0 \tag{6}$$

where $N = G + L_F K_i K_d C G_s G_i L_q$ and $R = L_F K_i K_p G_s G_i L_q - L_F K_s L_q$. The state space equation of the system can be obtained as

$$\dot{p} = Ap \tag{7}$$

where $p = (\dot{q}, q)^T$ and

$$A = \begin{bmatrix} -M^{-1}N & -M^{-1}R \\ I & O \end{bmatrix} \tag{8}$$

Under dynamic condition, the flywheel speed has $\Omega \neq 0$. Suppose that the flywheel is under the decentralized PID control ($C = C_d = I$). When the flywheel speed increases from $0\ Hz$ to $500\ Hz$, the eigenvalues of matrix A change with the flywheel speed. During the entire acceleration period, matrix A has two negative real eigenvalues and two pairs of conjugate eigenvalues. The negative real eigenvalues, $a_1^d = -138.87$ and $a_2^d = -99.51$, remain unchanged. However, the two pairs of conjugate eigenvalues, a_{3i}^d and $a_{4i}^d (i = 1,2)$, are greatly affected by the flywheel speed, as shown in Fig 3.

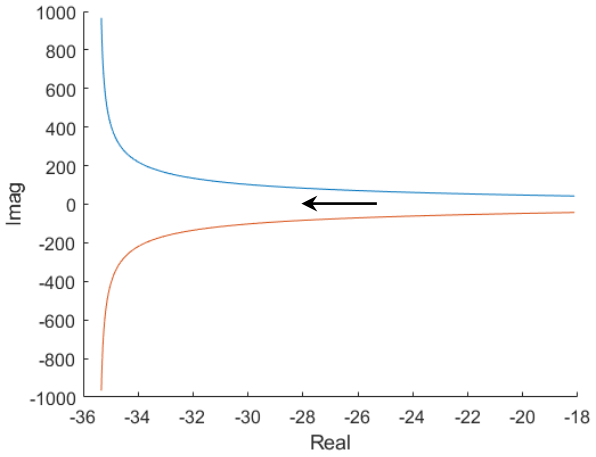

(a) a_{3i}^d

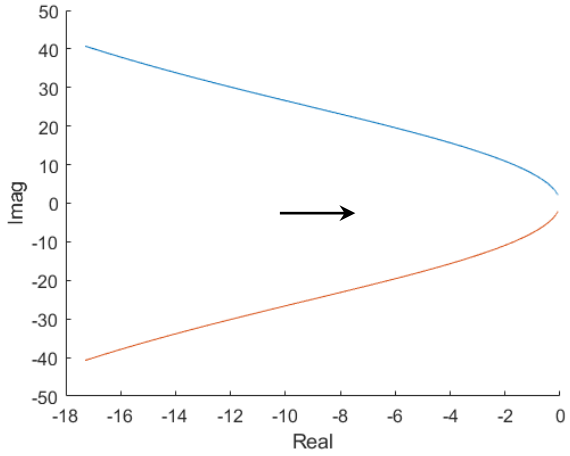

(b) a_{4i}^d

Figure 3. The conjugate eigenvalues change as the flywheel speed up.

It can be seen that the conjugate eigenvalues are affected by the speed. As the flywheel speeds up, a_{3i}^d moves away from the imaginary axis, while a_{4i}^d approaches the imaginary axis. Therefore, a_{4i}^d becomes the dominant eigenvalues for the system as the flywheel speeds up. Although a_{3i}^d and a_{4i}^d still have negative real parts at different flywheel speed, the robustness of the AMB controller is greatly affected. The decentralized PID controller designed for static state will fail to meet the control requirement as the flywheel speed up.

When a_{4i}^d approaches the imaginary axis, the damping ratio and the absolute value of the real part decrease, which means that the same external disturbances will leading to severer vibration of the flywheel and the AMB-FS will return to steady state slowly. In other words, although the original PID controller possesses good robustness under static state, as the flywheel speeds up, the robustness of AMB controller and the stability of AMB-FS decrease rapidly due to the influence of gyroscopic effect.

B. Controller Design

In order to improve the stability of the high-speed AMB-FS, the decentralized PID control is combined with cross feedback control in the actual experiment. The cross feedback control suppresses the precession and nutation frequency by taking the displacement signal in the orthogonal direction as the feedback, as shown in Fig 4.

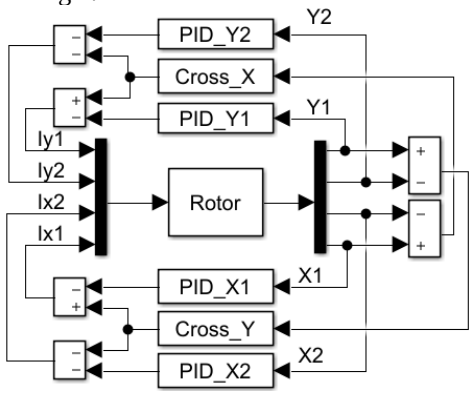

Figure 4. PID controller with cross feedback.

In order to suppress both the nutation and precession, it is necessary to add positive and negative displacement cross feedback simultaneously, and connect the low-pass and high-pass filters to the corresponding control channel. Therefore, the actual transfer function of the cross feedback is

$$G(s) = \frac{k_d}{T_{lp}s + 1} + \frac{k_{ch}s}{T_{hp}s + 1} \tag{9}$$

SIMULATION

The AMB-FS model is built in Matlab Simulink to observe the AMB-FS performance under the different PID controller. The model mainly includes flywheel module, cross feedback module and AMB module, as shown in Fig 5.

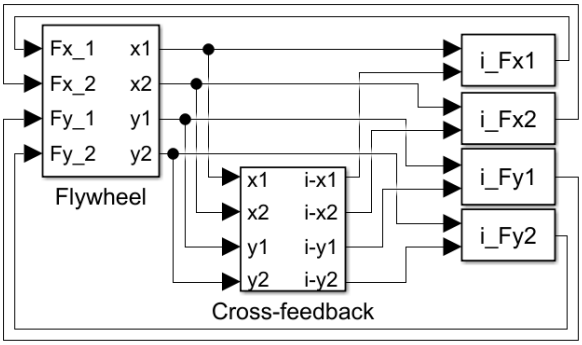

Figure 5. AMB-FS mode.

SIMULATION

A. Decentralized PID Controller

The AMB-FS is simulated under decentralized PID control. At 0.2 s, the flywheel is disturbed by the external force in the x direction at the position of MB_1. As shown in Fig 6, when the flywheel speed is only 25 Hz, the AMB-FS is unstable. Due to the gyroscopic effect of the flywheel, the external disturbance loaded in the x direction leads to the flywheel unstable both in the x and y directions. Therefore, merely very low flywheel speed will lead to strong gyroscopic effect and reduce the robustness of AMB controller greatly, which is consistent with the theoretical analysis.

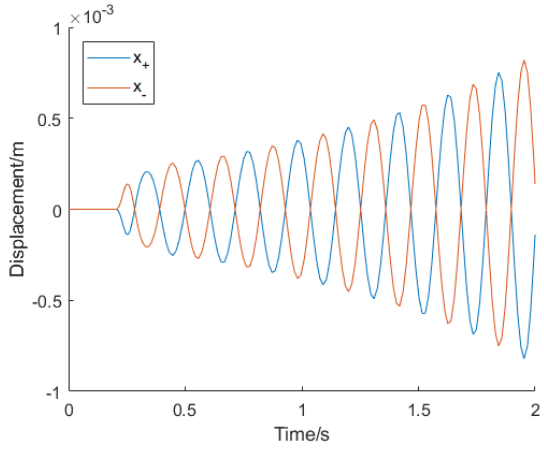

(a) Displacement in x direction

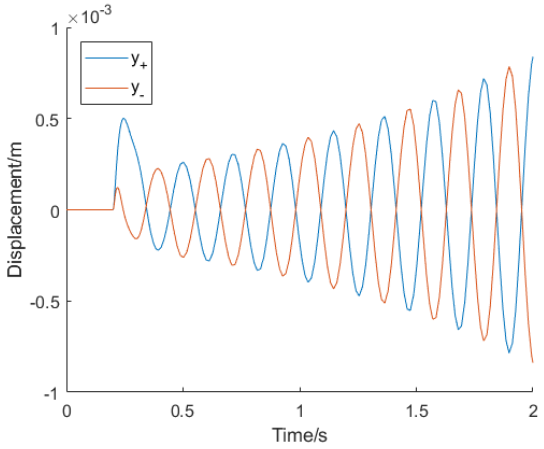

(b) Displacement in y direction

Figure 6. Displacements in x and y directions without cross feedback when the flywheel speed is 25Hz.

B. *Cross feedback PID Controller*

Under cross feedback PID control, the flywheel is loaded with the same external disturbance. As shown in Fig 7, the flywheel returns to steady state immediately in x direction, and there is no displacement in y direction. The flywheel has the same motion state when the flywheel speed is 25Hz and 500Hz, and the stability of the AMB-FS is good.

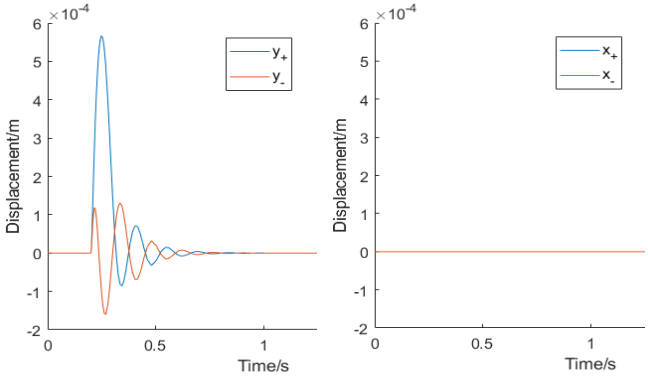

(a) Displacement in x direction (b) Displacement in y direction

Figure 7. Displacements in x and y directions with cross feedback when the flywheel speed is 25Hz and 500Hz.

It shows that the cross feedback can effectively suppress the gyroscopic effect of the flywheel, and the performance of AMB controller will not be affected. The x and y directions are decoupled, so the y direction will not be affected by the external disturbance in the x direction.

C. *Stability under Rotating Frame*

The rotating frame will lead to strong gyroscopic effect of the flywheel, so the AMB-FS is simulated in the rotating frame to observe the features of the AMB.

In the simulation, the flywheel rotates at the rated speed of 500 Hz, and the frame rotational speed gradually increases from 0 deg/s to 3.5 deg/s. Fig 8 shows the simulation results of frame rotational speed and the AMB forces.

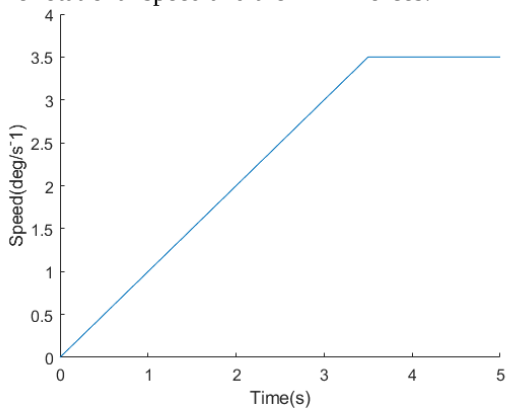

(a) Frame rotational speed

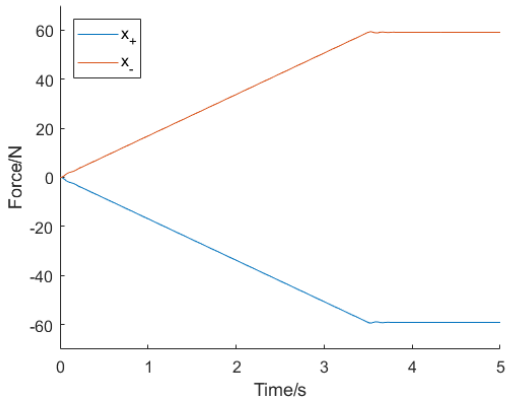

(b) AMB forces in x direction

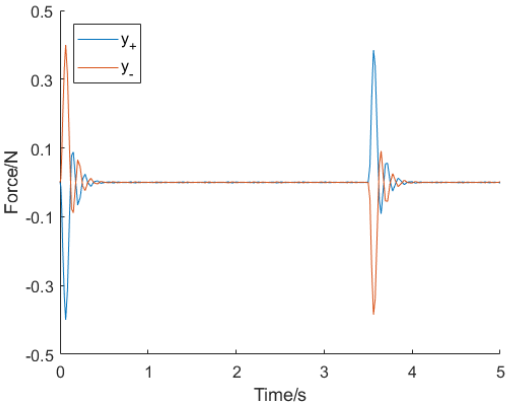

(c) AMB forces in y direction

Figure 8. Frame rotational speed and AMB forces.

According to theoretical analysis, when the frame rotates in the x direction, the AMB will generate force in x direction to suppress the gyroscopic effect of the flywheel. As shown in Fig 8(b), the AMB electromagnetic forces in x direction increase with the increase of frame rotational speed, and the force direction of two AMB is opposite. While in the y direction there is only a certain exciting force in the start and stop state of the frame acceleration. In the simulation, the frame rotational speed is reflected by the flywheel rotating in x direction. Therefore, there is no AMB force in the y direction during the frame acceleration.

EXPERIMENT

Fig 9 shows the AMB-FS experiment platform. The vertical AMB-FS is placed in the frame, and the frame is placed on the rotatable base. During the running of the AMB-FA, the frame can rotate in the x direction.

(a) Flywheel

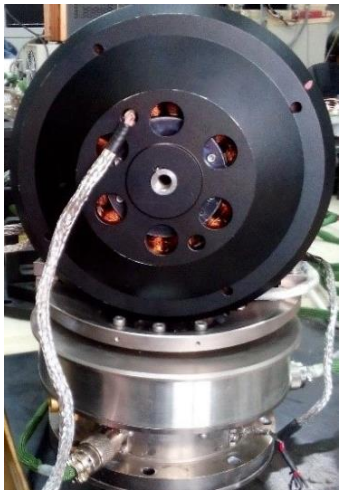

(b) AMB-FS on the rotatable base

Figure 9. Experiment platform.

A. *Static Suspension*

Fig 10 shows the axis orbit of the flywheel in static suspension. It can be seen that the AMB can suspend the flywheel stably in the static state, and the radial displacement of the flywheel is less than 1 um.

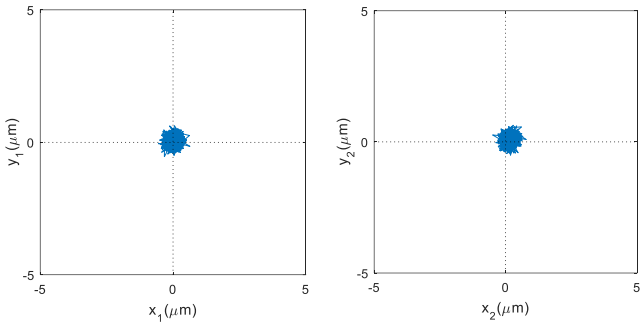

(a) Displacement at MB_1 (b) Displacement at MB_2

Figure 10. Axis orbit of the flywheel in static suspension.

B. *Gyroscopic effect suppression*

When the flywheel speed is high, the precession frequency gradually drops to zero, and the nutation frequency increases continually. It is difficult for the decentralized PID controller to effectively suppress the procession and nutation simultaneously. The performance of the cross feedback PID control on the gyroscopic effect is studied in the following experiment.

Fig 11 shows the axis orbit and displacement spectrum of the flywheel without cross feedback control. When the flywheel speed is 40Hz, the precession is unstable and the decentralized PID controller cannot provid enough damping for the precession mode.

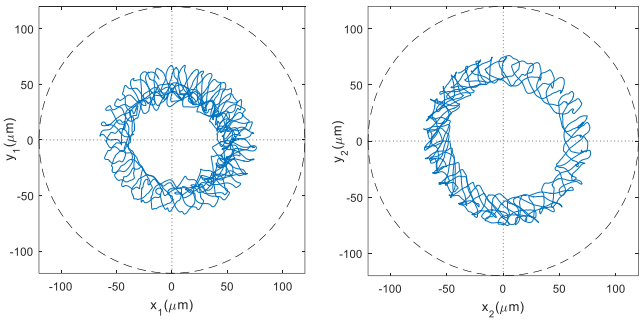

(a) Displacement at MB_1 (b) Displacement at MB_2

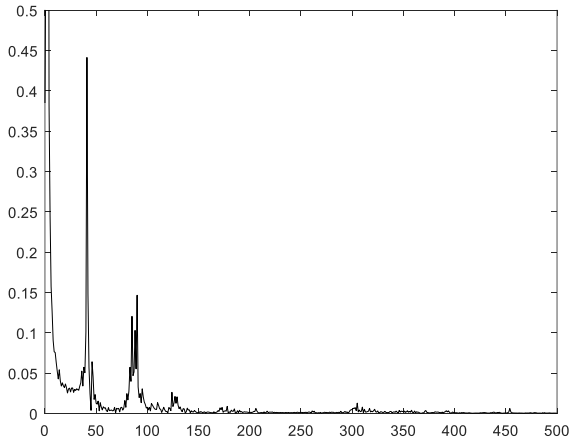

(c) Flywheel displacement spectrum

Figure 11. Precession instability.

Similarly, without cross feedback control, the nutation is unstable when the flywheel speed is 110 Hz, as is shown in Fig 12. The nutation frequency is 210 Hz, and the ratio between the

nutation frequency and the rotor speed is 1.91 , which is basically equal to the inertia ratio of the flywheel [17].

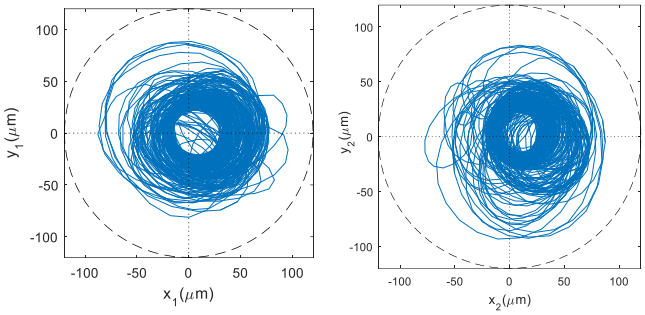

(a) Displacement at MB_1 (b) Displacement at MB_2

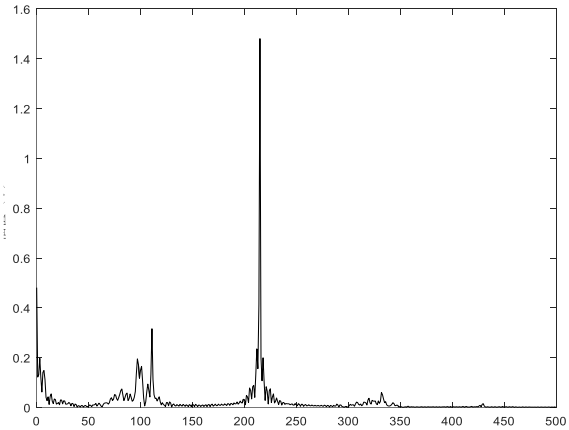

(c) Flywheel displacement spectrum

Figure 12. Nutation instability.

In order to effectively suppress the nutation and precession modes of the flywheel simultaneously, the cross feedback control was introduced. The speed-up experiment of AMB-FS is carried out after selecting the appropriate parameters for the cross feedback PID controller. Fig 13 shows the axis orbit and displacement spectrum of the flywheel. It can be seen that under cross feedback PID control, the procession and nutation modal frequencies are effectively suppressed simultaneously. The AMB controller shows good performance and the AMB-FS is highly stable.

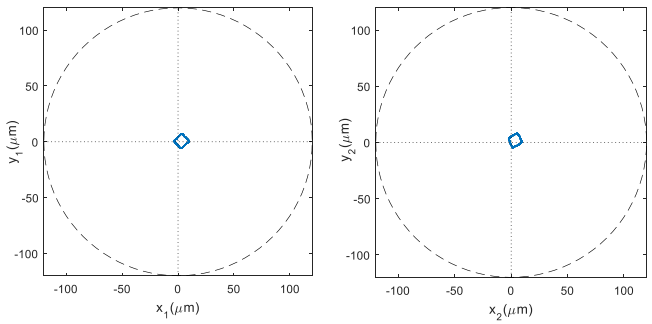

(a) Displacement at MB_1 (b) Displacement at MB_2

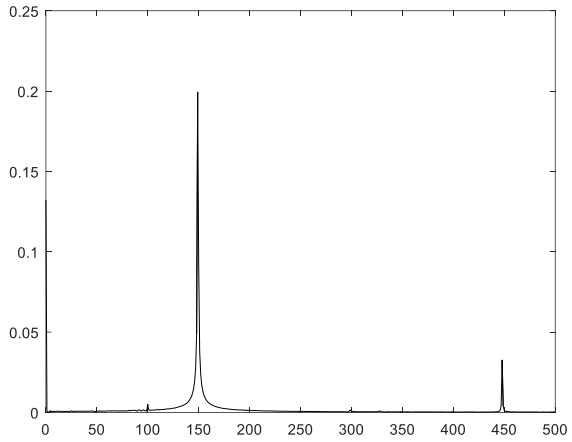

(c) Flywheel displacement spectrum

Figure 13. Stable suspension with cross feedback.

Under the cross feedback PID control, the flywheel speed could exceed 31200 rpm and still possess the speeding potential. When the flywheel rotates at the rated speed of 500Hz in the vacuum environment, the AMB-FS has the power consumption of 17.82W and needs no cooling measures. The radial vibration amplitude of the flywheel is less than 2μm, and the shaking intensity of the AMB-FS base is less than 0.016mm/s.

C. Rotating frame experiment

From the theoretical analysis above, it can be seen that the rotating frame leads to strong gyroscopic effect of the flywheel at high speed, which will reduce the AMB controller performance significantly. The flywheel may collide with the touchdown bearings, leading to the instability of the AMB-FS. Therefore, in the rotating frame, the stability of the AMB-FS is analyzed in the experiment.

In the experiment, the flywheel is suspended stably at the rated speed of 500Hz, and the frame rotates in the x direction at different angular velocity. The axial orbit of both ends of the flywheel and the flywheel displacement spectrum is shown in Fig 14, where the angular velocity of the frame is 1 deg/s, 1.5 deg/s and 2.5 deg/s, respectively.

From the experimental results, it can be seen that the increase of the frame rotational speed has no effect on the stability of the AMB-FS. There is little change in the flywheel axis orbit and the displacement spectrum. It proves that the cross feedback PID controller possesses good robustness and has high performance in resisting the disturbance of the rotating frame. The dynamic stability of the ultra-high AMB-FS is fully verified under the disturbance of the rotating frame in the experiment.

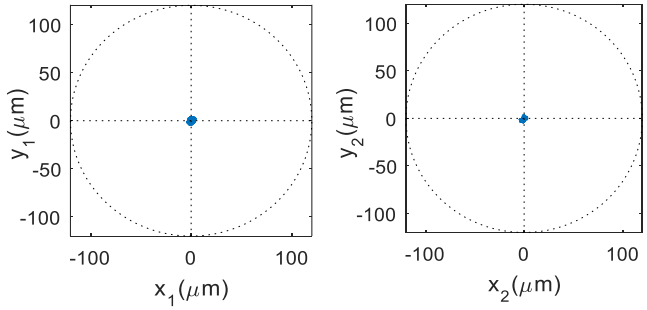

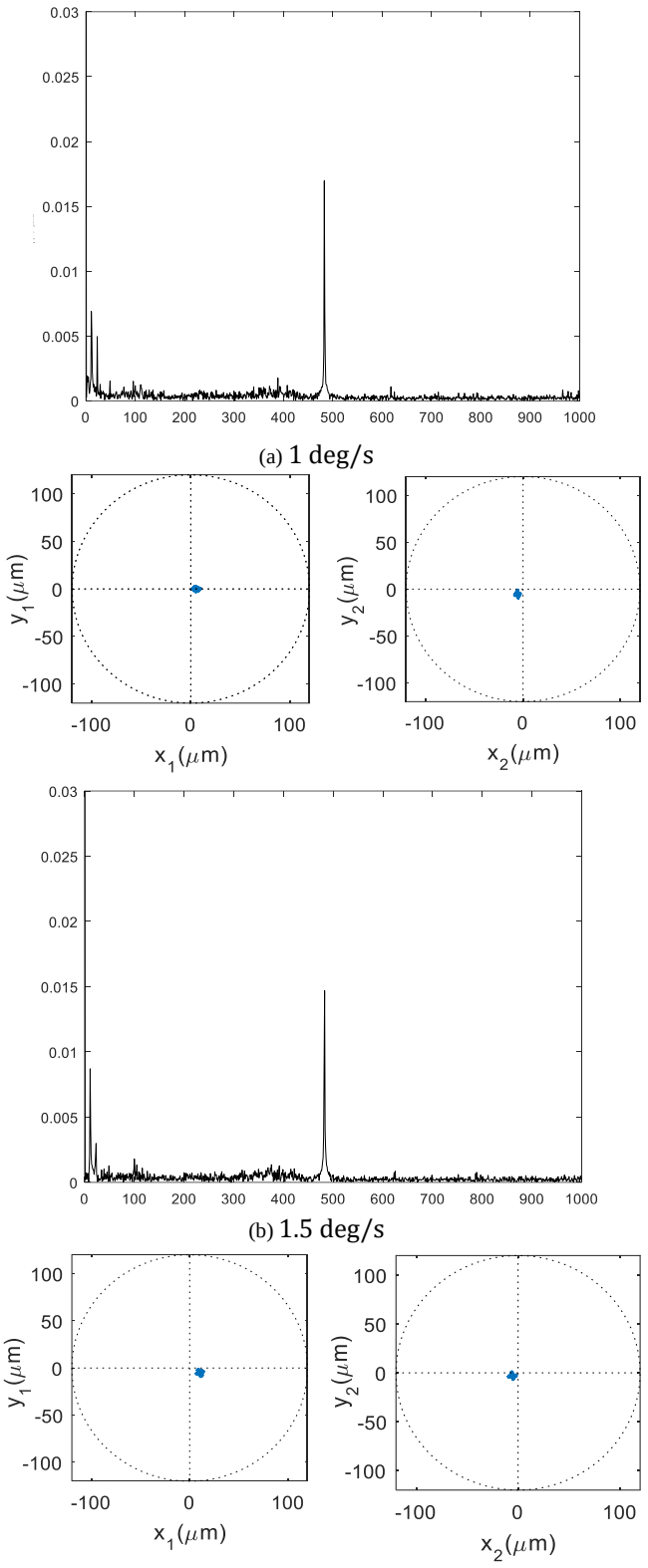

(a) 1 deg/s

(b) 1.5 deg/s

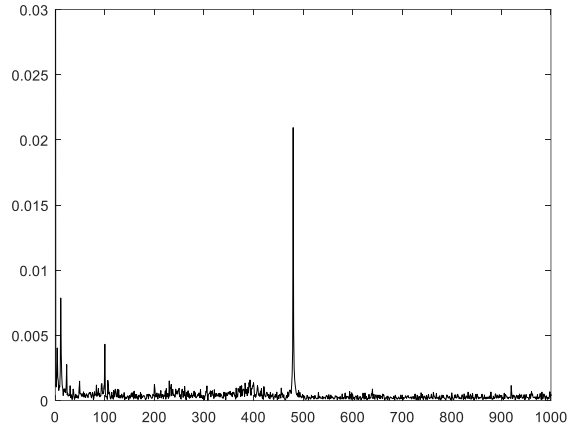

(c) 2.5 deg/s

Figure 14. Axis orbit and frequency spectrum of the flywheel displacement without cross feedback control.

D. Ultimate Performance experiment

Influenced by the gyroscopic effect and limited by the maximum AMB force, the frame rotational speed has different limit at different flywheel speed, which is verified in the following experiment.

Increase the frame rotational speed at a certain flywheel speed. When the flywheel vibrates violently, record the frame rotational speed as the maximum speed. Repeat the experiment at different flywheel speeds. Fig 15 shows the relationship between the flywheel speed and the maximum frame rotational speed. As the flywheel speed increases, the maximum frame rotational speed decreases rapidly. The ultimate performance experiment shows that the maximum frame speed can reach 3.5 deg/s at the rated flywheel speed of 500 Hz.

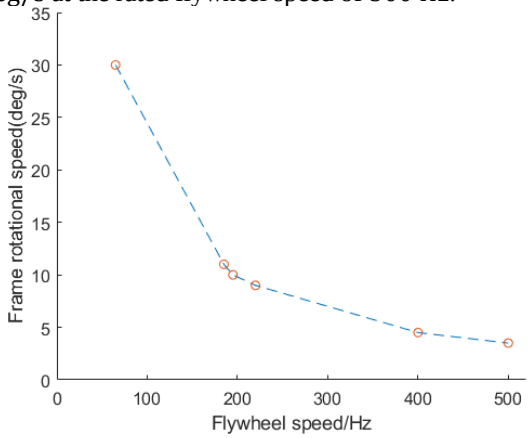

Figure 15. Relationship between flywheel speed and frame rotational speed.

The experimental results show the high stability of the AMB-FS at high flywheel speed. In the experiment, the AMB needs to provide extra force to offset the flywheel gravity. Therefore, if the flywheel is placed horizontally or in the microgravity, the robustness of AMB controller and the ultimate performance of AMB-FS will be further improved.

The performance of the AMB controller is important for the stability of the AMB-FS under the disturbance of rotating frame. Appropriate optimization of the controller parameters and proper distribution of the AMB force can further improve the

stability of the AMB-FS and the performance of AMB controller.

CONCLUSION

In this paper, through the external disturbance analysis, AMB controller design, simulation and stability experiment, the AMB-FS is designed and studied, and the system stability is analyzed in the experiment.

Through stability experiment of the high-speed AMB-FS, various ultimate performance of the system in the rotating frame are studied:

- Under cross feedback PID control, the gyroscopic effect of the flywheel is effectively suppressed.
- The flywheel can be suspended stably at any speed within the range of 0 to 30000 rpm in the vacuum environment, and the AMB-FS shows high stability.
- The flywheel speed could exceed 31200 rpm and still possess the speeding potential.
- When the flywheel rotates at the rated speed of 500 Hz in the vacuum environment, the AMB-FS has the power consumption of 17.82 W and needs no cooling measures.
- The radial vibration amplitude of the flywheel is less than 2 μm, and the shaking intensity of the AMB-FS base is less than 0.016 mm/s.
- The maximum frame rotational speed at different flywheel speeds is analyzed, and the maximum frame speed can reach 3.5 deg/s at the rated flywheel speed of 500 Hz.

In order to improve the system performance, further research can be implemented with the following points. Analyze the influence of the coupled electromagnetic field between the AMB and the drive motor with the accurate finite element analysis. Study the influence factor of the resistance moment for further reducing the energy loss of the high-speed AMB-FS. Design low power AMB controller to further reduce the system power consumption.

REFERENCES

[1] Z. Kai, D. Xingjian, and Z. Xiaozhang, “Dynamic analysis and control of an energy storage flywheel rotor with active magnetic bearings,” *2010 International Conference on Digital Manufacturing Automation*, vol. 1, pp. 573–576, Dec 2010.

[2] S. Zheng, H. Li, B. Han, and J. Yang, “Power consumption reduction for magnetic bearing systems during torque output of control moment gyros,” *IEEE Transactions on Power Electronics*, vol. 32, no. 7, pp. 5752–5759, July 2017.

[3] M. Andriollo, E. Scaldaferro and A. Tortella, "Design optimization of the magnetic suspension for a flywheel energy storage application," *2015 International Conference on Clean Electrical Power (ICCEP)*, Taormina, 2015, pp. 216-221, 2015.

[4] Qunming Li, Songduo Yin, Liang Wan and Ji'an Duan, "Stability Analysis and Controller Design for a Magnetic Bearing with 5 Degree of Freedoms," *2006 6th World Congress on Intelligent Control and Automation*, Dalian, pp. 8015-8019, 2006.

[5] Pu, Peng Cheng, J. P. Yu, and L. Zhao. "Analysis of Stiffness and Damping Properties of Active Magnetic Bearing Using Cross Feedback Control." *International Conference on Mechanics and Mechanical Engineering* 2017.

[6] M. Ahrens, L. Kucera and R. Larsonneur, "Performance of a magnetically suspended flywheel energy storage device," *IEEE Transactions on Control Systems Technology*, vol. 4, no. 5, pp. 494-502, Sep 1996.

[7] Kai, Z., Lei, Z., & Zhao, H. Research on control of flywheel suspended by active magnetic bearing system with significant gyroscopic effects. *Chinese Journal of Mechanical Engineering*, pp. 63-66, 2004.

[8] Huidong G. Research of active magnetic bearing-flexible rotor system. *Department of Engineering Phisics, Tsinghua University*, 2005.

[9] Zhang, K., Zhu, R., & Zhao, H. Experimental research on a momentum wheel suspended by active magnetic bearings. *Proceedings of the 8th ISMB, Mito*, pp. 605-609, 2002.

[10] Horiuchi, Y. Development of magnetic bearing momentum wheel for ultra-precision spacecraft attitude control. *7th Int. Symposium on Mognetic Bearings*, pp. 525-530, 2000.

[11] Li, G., Allaire, P. E., Lin, Z., & Huang, B. (2002, August). Dynamic transfer of robustness AMB controllers. *8th International Symposium on Magnetic Bearings, Mito, Japan*, pp. 471-476, Aug 2002.

[12] Sivrioglu, S. Lmi based gain scheduled h ∞ controller design for amb systems under gyroscopic and unbalance disturbance effect. *Proc.int.symp.on Magnetic Bearings*, pp. 191-196, 1996.

[13] F. Matsumura, T. Namerikawa, K. Hagiwara and M. Fujita, "Application of gain scheduled H_∞ robustness controllers to a magnetic bearing," in *IEEE Transactions on Control Systems Technology*, vol. 4, no. 5, pp. 484-493, Sep 1996.

[14] Tsiotras, P., & Mason, S. Self-scheduled H∞ controllers for magnetic bearings. In *International Mechanical Engineering Congress and Exposition, Atlanta, GA*, pp. 151-158, Nov 1996.

[15] Hawkins L A, Murphy B T, Kajs J. Analysis and testing of a magnetic bearing energy storage flywheel with gain-scheduled, MIMO control. *Proceedings of ASME Turbo Expo, Munich, Germany*, pp. 173-179, 2000.

[16] Gang, T. X. F. J. L. Gain scheduling cross feedback control approach for magnetic suspending flywheel. *Journal of Beijing University of Aeronautics and Astronautics*, pp. 1299-1303, 2006.

[17] Jiancheng F. Technology of magnetic suspension control moment gyroscope. *Nationnal defense industry press*, 2012.